

ПРОЕКТУВАННЯ І МАТЕМАТИЧНЕ МОДЕЛЮВАННЯ СЕНСОРІВ

SENSORS DESIGN AND MATHEMATICAL MODELING

UDC 681.7.068.4

MODELING OF LONG-PERIOD FIBER GRATINGS AND THEIR APPLICATION ON LIQUID LEVEL SENSORS

(За матеріалами доповіді на конференції СЕМСТ-2)

I. Flores-Llamas and V. Svyryd

Faculty of Engineering, National Autonomous University of Mexico
C.U., Mexico D.F., C.P. 04510, Tel. +52(55) 5622 3060, Fax: +52(55) 5616 1855
e-mail: ifloresllamas@yahoo.com, vladimirsk@hotmail.com

Abstract

MODELING OF LONG-PERIOD FIBER GRATINGS AND THEIR APPLICATION ON LIQUID LEVEL SENSORS

I. Flores-Llamas and V. Svyryd

It is presented a mathematical model for non-uniform long-period fiber gratings which is based on the Coupled-Mode Theory. The model has the capability of considering the case of a surrounding medium with a refractive index higher than that of the optical fiber cladding, which gives advantages in a number of applications. As an application of the model a new liquid level sensor is proposed and the results of its simulation are compared with experimental data.

Keywords: long period fiber gratings, refractometry, liquid level sensors.

Резюме

МОДЕЛЮВАННЯ ДОВГОПЕРІОДНИХ ВОЛОКОННО-ОПТИЧНИХ РЕШІТОК ТА ЇХ ЗАСТОСУВАННЯ В СЕНСОРАХ РІВНЯ РІДИНИ

І. Флорес-Льямас, В. Свирид

Подана математична модель неоднорідної довгоперіодної волоконно-оптичної решітки, заснована на теорії зв'язаних мод. Ця модель здатна врахувати й випадок з показником заломлення навколишнього середовища вищим, ніж в оболонки оптичного волокна, що дає переваги в багатьох застосуваннях. В якості одного із застосувань моделі, розроблено новий сенсор рівня рідини, а також порівнюються результати його моделювання з експериментальними даними.

Ключові слова: довгоперіодні волоконно-оптичні решітки, рефрактометрія, сенсори рівня рідини.

Резюме**МОДЕЛИРОВАНИЕ ДЛИННОПЕРИОДНЫХ ВОЛОКОННО-ОПТИЧЕСКИХ РЕШЕТОК И ИХ ПРИМЕНЕНИЕ В ДАТЧИКАХ УРОВНЯ ЖИДКОСТИ***И. Флорес-Льямас, В. Свирид*

Представлена математическая модель неоднородной длиннопериодной волоконно-оптической решетки, основанная на теории связанных мод. Эта модель способна учесть и случай с коэффициентом преломления окружающей среды выше, чем у оболочки оптического волокна, что дает преимущества во многих применениях. В качестве одного из применений модели, разработан новый датчик уровня жидкости, а также сравниваются результаты его моделирования с экспериментальными данными.

Ключевые слова: длиннопериодные волоконно-оптические решетки, рефрактометрия, датчики уровня жидкости.

1. Introduction

Recently, long-period fiber gratings (LPFGs) have experienced a remarkable demand in optical communication devices and sensing systems applications. They show higher sensitivity with respect to temperature, strain-induced and external refractive index changes, than their counterparts fiber Bragg gratings; and some techniques have been employed in order to further increase this sensitivity. In particular, the change in the index of refraction of the external medium causes changes in the transmission spectrum response of LPFGs; this response depends on a combination of the grating parameters and has been determined both theoretically and experimentally.

LPFGs have been modeled accurately with the Coupled-Mode Theory (CMT), this theory allows us to consider several parameters of the gratings, for instance length of the grating, period chirp, apodization, etc. Since LPFGs are highly sensitive to the external medium, they have been employed as refractive index sensors. However, the applicability of these devices has been constrained to a reduced interval of the external refractive index, because their sensitivity decreases when the external index is higher than that of the cladding fiber. Furthermore, the properties of LPFGs, under the influence of a medium with high refractive index, have been investigated theoretically only by few authors [1, 2]. These works present well-defined models for uniform LPFGs under these circumstances, but in many cases non-uniform LPFGs, with certain apodization or period chirp, show some advantages, therefore, it is desirable to have an approach for modeling and simulating this kind of gratings.

In this work is presented a more complete and

versatile mathematical model for non-uniform LPFGs, which is based on the CMT and takes advantage of the F-matrix formalism. Besides, the mathematical model also considers the case of a surrounding medium with a refractive index higher than that of the optical fiber cladding, providing a wider working refractive index range, and giving further advantages in applications such as refractometric sensors, liquid level sensors, and tunable optical filters. Finally, in the present work is proposed a new liquid level sensor that operates properly for those cases when the refractive index of the liquid is higher than the refractive index of the fiber cladding. This liquid level sensor has been simulated with the described model and the results of its simulation coincide with experimental results.

2. Modeling of LPFGs

An LPFG is a periodic modulation of the effective refractive index of the fiber modes, there are several forms to produce this modulation, however, the most widely used consist in modifying the material refractive index by taking advantage of the fiber photosensitivity to the UV-radiation, or modifying the fiber diameter employing etching or heating technologies. LPFGs have a typical period in the range of 100 to 600 μm and, when induced in single-mode optical fibers, untilted gratings have the property of coupling light between the fundamental core mode (HE_{11}) and several cladding modes of different order and with the same azimuthal symmetry (HE_{1l}). The complex amplitudes of the modes are related by the well-known coupled equations for co-propagating modes

$$\frac{dA(z)}{dz} = j\sigma_A A(z) - j\kappa B(z), \quad (1)$$

$$\frac{dB(z)}{dz} = j\sigma_B B(z) - j\kappa^* A(z), \quad (2)$$

where $A(z)$ is the core mode amplitude, $B(z)$ is the cladding mode amplitude, κ is the ac cross-coupling coefficient, and σ_A and σ_B are general dc self-coupling coefficients of the core and cladding modes respectively. In general σ_A and σ_B are different because the propagation conditions of the core and cladding modes may be distinct, thus they are defined by

$$\sigma_A = \delta + \sigma_{co}, \quad (3)$$

$$\sigma_B = \delta + \sigma_{cl}, \quad (4)$$

where it is assumed that there is no chirp in the grating and δ is the detuning given by

$$\delta = \frac{1}{2}(\beta_{co} - \beta_{cl,i}) - \frac{\pi}{\Lambda}, \quad (5)$$

here β_{co} and $\beta_{cl,i}$ are the core mode and cladding mode propagation constants respectively, and Λ is the grating period. Also in Eqs. (3) and (4), σ_{co} and σ_{cl} are dc self-coupling coefficients of the core and cladding modes respectively, and their value is determined by the mode overlap integral. In order to determine β_{co} , the eigenvalue equation for a step-index fiber and for HE modes must be solved [3], and if the effect of the core on the propagation constant of cladding HE_{1i} modes is neglected, the same eigenvalue equation may be employed to calculate $\beta_{cl,i}$.

When the external index n_3 is higher than the cladding index n_2 , the cladding fiber and the external medium can be considered as a hollow or leaky waveguide [4]. For this type of waveguide there is no total internal reflection, cladding modes experience Fresnel reflection at the boundary between the two media instead, giving rise to losses in the different cladding modes. In this case the eigenvalue equation still holds provided that $\beta_{cl,i}$ and other quantities take complex values [4]; the real part of $\beta_{cl,i}$ represents the phase velocity and its imaginary part represents the loss rate. The solution of the eigenvalue equation becomes rather complex when the arguments of the Bessel functions take complex values, however, under the restrictions of low-loss cladding modes and wavelength much less than the cladding radius, the complex propagation constant is approximated by [4]

$$\beta_{cl,i} = \left[k_0^2 n_2^2 - \left(\frac{u^{(1)}}{a_2} \right)^2 \right]^{1/2}, \quad (6)$$

where

$$u^{(1)} \approx u^{(0)} \left[1 - \frac{j(n_3^2 + n_2^2)}{2a_2 k_0 n_2^2 (n_3^2 - n_2^2)^{1/2}} \right], \quad (7)$$

$u^{(0)}$ is the zero-order real approximation for the parameter u given by the i^{th} root of

$$J_{l-1}(u^{(0)}) = 0 \text{ for HE}_{li} \text{ modes}, \quad (8)$$

k_0 is the free-space propagation constant, and a_2 is the cladding radius.

This analysis indicates that σ_B is complex-valued when the fundamental core mode couples to leaky cladding modes, because the imaginary part of $\beta_{cl,i}$ must be incorporated to σ_{cl} since, by definition, δ is a real quantity, which measures the deviation of the wavelength from the resonant wavelength of the grating.

An appropriate and straightforward approach for modeling non-uniform LPFGs is the F-matrix formalism [5], in which the grating is divided into M sections, each having constant parameters and being characterized by a 2×2 matrix F_m . Assuming that the grating extends from 0 to L along the axis z and one grating section m extends from $z = z_{m-1}$ to $z = z_m$, the amplitudes of the modes at the section boundaries are related by

$$\begin{bmatrix} R(z_m) \\ S(z_m) \end{bmatrix} = F_m \begin{bmatrix} R(z_{m-1}) \\ S(z_{m-1}) \end{bmatrix}, \quad (9)$$

where the elements of the fundamental matrix for section m , obtained from Eqs. (1) and (2) and applying appropriate boundary conditions, are given by

$$F_{m,11} = \frac{1}{\gamma_1 - \gamma_2} [(\sigma_A - \gamma_2) \exp(j\gamma_1 L_m) + (\gamma_1 - \sigma_A) \exp(j\gamma_2 L_m)], \quad (10)$$

$$F_{m,12} = \frac{-\kappa_m}{\gamma_1 - \gamma_2} [\exp(j\gamma_1 L_m) - \exp(j\gamma_2 L_m)], \quad (11)$$

$$F_{m,21} = \frac{-(\gamma_1 - \sigma_A)(\sigma_A - \gamma_2)}{\kappa_m(\gamma_1 - \gamma_2)} [\exp(j\gamma_1 L_m) - \exp(j\gamma_2 L_m)], \quad (12)$$

$$F_{m,22} = \frac{1}{\gamma_1 - \gamma_2} [(\gamma_1 - \sigma_A) \exp(j\gamma_1 L_m) + (\sigma_A - \gamma_1) \exp(j\gamma_2 L_m)], \quad (13)$$

here

$$\gamma_1 = \frac{(\sigma_A - \sigma_B) + \sqrt{(\sigma_A - \sigma_B)^2 + (\kappa_m^2 + \sigma_A \sigma_B)}}{2}, \quad (14)$$

$$\gamma_2 = \frac{(\sigma_A - \sigma_B) - \sqrt{(\sigma_A - \sigma_B)^2 + 4(\kappa_m^2 + \sigma_A \sigma_B)}}{2}, \quad (15)$$

$L_m = z_m - z_{m-1}$, and κ_m is the ac cross-coupling coefficient in section m . Finally, the single 2×2 matrix F that describes the complete LPFG is obtained by multiplying the M matrices of each section, so the output mode amplitudes are calculated from

$$\begin{bmatrix} R(L) \\ S(L) \end{bmatrix} = F \begin{bmatrix} R(0) \\ S(0) \end{bmatrix}. \quad (16)$$

3. Design of liquid level sensors

In an LPFG cladding modes show high sensitivity to the changes of the external index, hence, any variation of the external medium refractive index, in the grating region, causes changes on the resonant or central wavelength of the LPFG. This central wavelength of the attenuation bands in a uniform LPFG can be obtained from Eq. (5) and is given by

$$\lambda_i = (n_{co}^{eff} - n_{cl,i}^{eff})\Lambda, \quad (17)$$

where n_{co}^{eff} and $n_{cl,i}^{eff}$ are the effective indexes of the core mode and cladding mode of order i respectively. The sensitivity of the grating is determined by its period and the order of the cladding mode. Furthermore, for values of n_3 between air and n_2 , λ_i decreases as n_3 increases; but when n_3 is equal to n_2 , the attenuation band disappears, and for values of n_3 higher than n_2 , the attenuation band reappears at a λ_i somewhat higher than that when the fiber is surrounded by air, but with smaller depth of the transmission minimum. This behavior can be exploited to measure the level of liquids with certain refractive index.

A liquid level sensor has been presented in [6], its principle of operation consists in measuring the minimum transmission value of the two attenuation bands that appear when a uniform LPFG is partially immersed in a liquid with a refractive index almost equal but lower than that of the fiber cladding. In this case the grating can be considered as two cascaded gratings, each with different attenuation bands and, consequently, different central wavelengths. However, such attenuation bands may overlap if they are wide enough and one grating is surrounded by air and

the other by a medium with refractive index close to the index of air or higher than the cladding index. Furthermore, the minimum value of the transmission and the attenuation bandwidth of each grating depend upon its length which is proportional to the liquid level; but its central wavelength does not vary if this length is modified.

In contrast, here is proposed a liquid level sensor based on the variation of the central wavelength λ_i , of a chirped LPFG, due to the level of a liquid h , with a refractive index n_{liq} higher than that of the fiber cladding. According to Eq. (17), a method to produce a shift in the central wavelength of each grating region (immersed and not immersed), as the liquid level changes, is to introduce a period chirp in the whole physical grating. Although the central wavelength of a chirped LPFG cannot be found with Eq. (17), because the parameters change along the grating, the equation suggests that, in certain degree, λ_i is proportional to the average period; as a result, the λ_i of each grating must suffer a shift if its effective length changes. Finally, the transmission spectrum and λ_i of the two cascaded LPFGs may be calculated making use of the F-matrix approach [7].

4. Results of simulation and experiment

A chirped LPFG, fabricated in a single-mode optical fiber (SMF-28), was simulated in order to obtain the variation of the central wavelength for the 4th order cladding mode. The fiber has the following parameters: core radius of 4.0 μm , cladding average radius in the region of the grating of 61.0 μm , and refractive index difference of 0.34 %. And the grating parameters are as follows: total length $L \approx 23.6$ mm, ac cross-coupling coefficient $\kappa = 0.66 \text{ cm}^{-1}$, a period which varies linearly from 490.8 to 491.9 μm , and the grating was divided into $M = 12$ sections. A schematic diagram of the configuration of the liquid level sensor is illustrated in Fig. 1, the grating was placed in a liquid container with its end of minimum period (490.8 μm) as the point of $h = 0$ mm, a broad band light source was coupled to one end of the fiber and an optical spectrum analyzer to the other end.

The transmission spectra of this liquid level sensor were calculated for different level values of a liquid with a refractive index of $n_{liq} = 1.454$ (refractive index difference $n_{liq} - n_2 \approx 0.009$) and they are shown in Fig. 2. This figure presents the calculated transmission spectra and shows that not only the minimum transmission value and the width, but

also the central wavelength of the attenuation band change. On one hand, the changes in the minimum transmission value and width are mainly due to the decreasing effective length of the LPFG region surrounded by air as the liquid level increases, in this case the effect of the grating region under the influence of n_{liq} is rather weaker compared to the effect of the other grating region. On the other hand, the reason why the central wavelength shifts is the change in the average period of the LPFG region which remains in air as the liquid level increases.

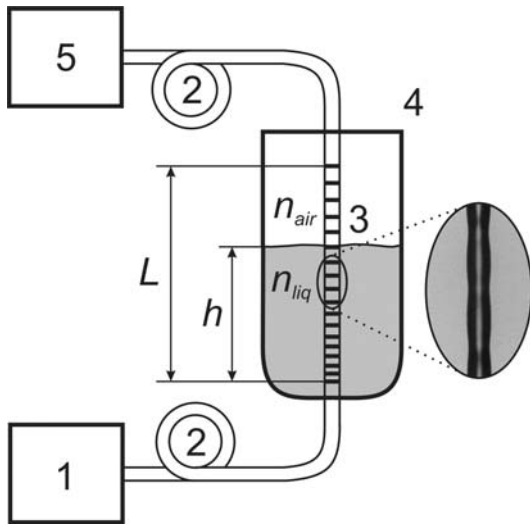


Fig. 1. Configuration of the liquid level sensor: optical source (1), optical fiber (2), chirped LPFG (3), liquid container (4), and optical spectrum analyzer (5).

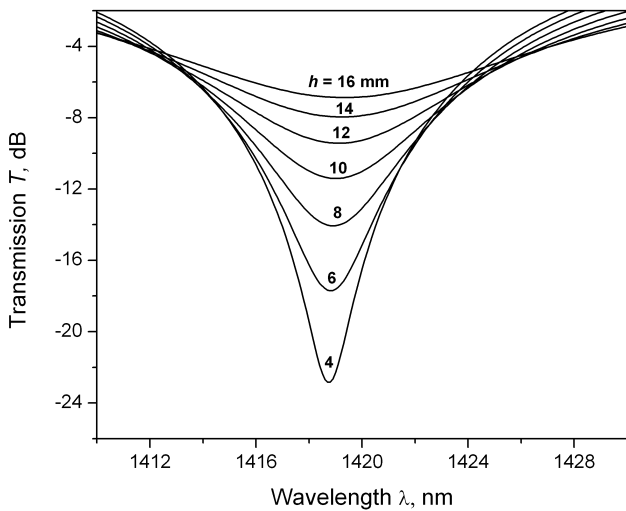


Fig. 2. Transmission spectra of the chirped LPFG calculated for different level values h .

An LPFG, with the parameters mentioned above, was fabricated using the point-by-point technique and by heating the optical fiber with a focused beam of a CO₂ laser, in a similar manner as the one described and employed in [8]. Then, the grating was placed as indicated in Fig. 1 and the transmission spectra was measured with an optical spectrum analyzer for the same index difference $n_{liq} - n_2$ and the same liquid level values of the simulation described above. The results are shown in Fig. 3. It can be observed that the behavior of the practical level sensor coincides with the behavior predicted by the simulation, there is a change in the minimum transmission value, width, and central wavelength of the attenuation band as the liquid level is increased.

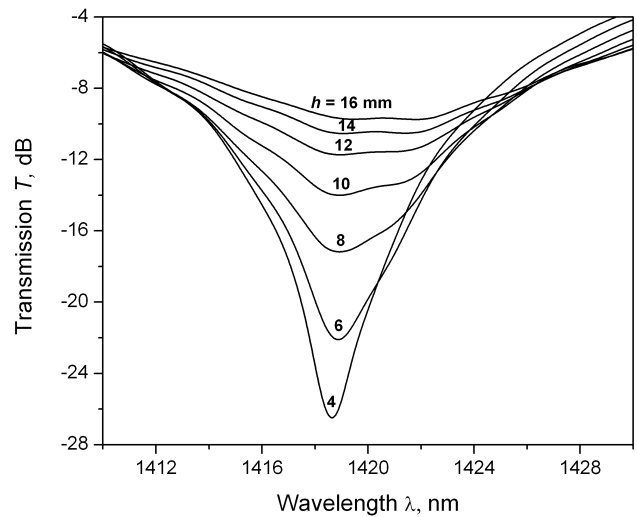


Fig. 3. Transmission spectra of the chirped LPFG measured for different level values h .

The variation of λ_i for this liquid level sensor was obtained theoretically and experimentally, and it is illustrated in Fig. 4 (λ_i corresponds to the minimum value of the transmission spectra). The shape of the calculated function $\lambda_i(h)$ coincides with the experimental data: for low liquid level $h \leq 4$ mm and high liquid level $h \geq 16$ mm the slope takes a small value, it increases within the interval of h from 4 to 16 mm. Also, it can be noticed that the interval of linearity is for $4 \leq h \leq 16$ mm, in which the slope has an approximate value of 0.05 nm/mm. On the other hand, we believe that the discrepancies between the calculated and experimental results arise from certain lack of precision in the value of κ , since the technology employed to fabricate the grating is not optimal at the moment.

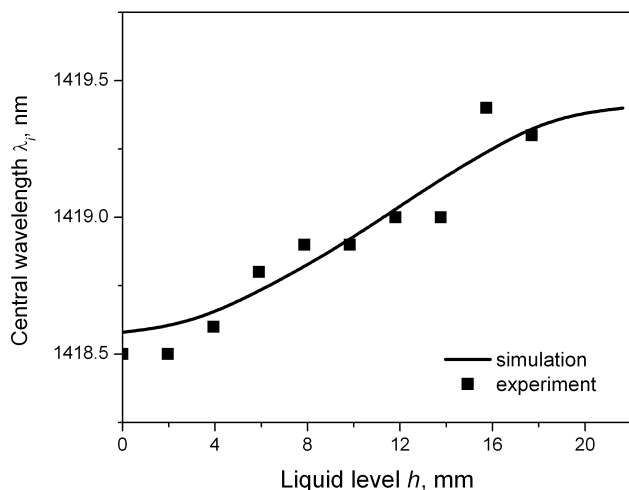


Fig. 4. Theoretical and experimental data of the central wavelength λ_p , as function of the liquid level h .

5. Conclusions

The more general model for LPFGs presented in this work is useful for calculating the transmission spectrum and the central wavelength of non-uniform gratings under the influence of an external medium with refractive index lower and higher than the fiber cladding index, this model is simple and takes advantage of some approximations valid for hollow or leaky waveguides. In addition, the introduced liquid level sensor, based on a non-uniform (chirped) LPFG, changes its central wavelength as the liquid level increases, showing a reasonable range of linearity.

Acknowledgment. The authors would like to thank the support of the DGAPA (PAPIIT, IN104302 and IN109406 research grants) of the National Autonomous University of Mexico, for this investigation.

References

1. Koyamada Y., Numerical analysis of core-mode to radiation-mode coupling in long-period fiber gratings // *IEEE Photon. Technol. Lett.* — 2001. — Vol.13, No.4. — P.308-310.
2. Hou R., Ghassemlooy Z., Hassan A. et al., Modeling of long-period fibre grating response to refractive index higher than that of the cladding // *Meas. Sci. Technol.* — 2001. — Vol.12. — P.1-5.
3. Yariv A., *Optical electronics in modern communications.* — New York: ed. by Oxford University Press, 1996. — 744 p.
4. Adams M.J., *An introduction to optical waveguides.* — New York: ed. by John Wiley & Sons, 1981. — 397 p.
5. Yamada M. and Sakuda K., Analysis of almost-periodic distributed feedback slab waveguides via a fundamental matrix approach // *Appl. Opt.* — 1987. — Vol.26 — P.3474-3478.
6. Khaliq S., James S.W., and Tatam R.P., Fiber-optic liquid-level sensor using long-period grating // *Opt. Lett.* — 2001. — Vol.26. — P.1224-1226.
7. Flores Llamas I., Kolokoltsev O., and Svyryd V., Refractometric sensors based on long period optical fiber gratings // *Rev. Mex. Fís.* — 2006. — Vol.S52, No.2. — P.75-78.
8. Chong J.H., Shum P., Haryono H. et al., Measurements of refractive index sensitivity using long-period grating refractometer // *Opt. Commun.* — 2004. — Vol.229. — P.65-69.